Signal Processing 93 (2013) 1921–1932

Contents lists available at SciVerse ScienceDirect

Signal Processing

journal homepage: www.elsevier.com/locate/sigpro

Genetic algorithm for rigid body reconstruction after micro-Doppler removal in the radar imaging analysis

LJubiša Stanković, Vesna Popović-Bugarin*, Filip Radenović

University of Montenegro, Electrical Engineering Department, Podgorica, Montenegro

ARTICLE INFO

Article history:
Received 16 July 2012
Received in revised form
15 October 2012
Accepted 4 January 2013
Available online 17 January 2013

Keywords:
Radar imaging
Micro-Doppler
L-statistics
Short-time Fourier transform
Genetic algorithm

ABSTRACT

Recently, an L-statistics based method for the micro-Doppler effects removal has been proposed by the authors. Order statistics is performed on the spectrogram, while the rigid body signal synthesis is done by using the remaining STFT samples, after micro-Doppler removal. By the proposed method, the Fourier transform is recovered with a concentration close to the original one. However, during the procedure of the micro-Doppler removal, the STFT samples that correspond to the rigid body are retracted, as well. Consequently, in the reconstructed Fourier transform of the rigid body, we get one very highly concentrated pulse, as in the original Fourier transform, and a number of low-concentrated components, being spread around the peak. These low concentrated components are summed up by different random phases. In this paper, we propose a genetic algorithm for the estimation of the removed STFT samples corresponding to the rigid body. Each individual in the genetic algorithm contains possible estimation of the phases of the missing STFT samples, whereas fitness function forces individuals (combination of phases) for which a minimal energy of the side lobs is obtained. The individual with the highest fitness is considered as the final phases' estimation of the missing STFT values, and then used for the reconstruction of the original Fourier transform. The amplitude of a STFT sample is estimated as median of the amplitudes of the remaining samples at the same frequency. Performance of the proposed genetic algorithm is illustrated by examples.

1. Introduction

Micro-Doppler (m-D) effect appears in the inverse synthetic aperture radar (ISAR) imaging when a target has one or more fast moving parts [1–7]. Similar effect appears in the synthetic aperture radar (SAR) imaging as well [8]. This effect may decrease readability of radar images by covering the rigid body and making it difficult to detect. Thus, the extraction of the m-D effect from the radar images has attracted significant research attention [9–14]. Recently, an effective and simple method for the m-D removal has been proposed in [15]. It is based on the L-statistics. In order to remove the m-D effect, the short time Fourier transform (STFT) is calculated within the coherent integration time (CIT). Then, the fact that a rigid body and fast rotating points behave differently in the time frequency (TF) plane is used for the m-D removal. Namely, the frequency content of an m-D signal is time variant and it covers a wide range of frequencies, but only for short time intervals. On the other hand, the frequency content of a rigid body return is almost constant in time. Consequently, in the STFT sorted along the time axis the m-D part of the signal has non-zero values over a wide frequency range, but only for a few samples in the sorted

* Corresponding author. Tel.: +382 20 245 839; fax: +382 20 245 873.
E-mail addresses: ljubisa@ac.me (L. Stanković), pvesna@ac.me (V. Popović-Bugarin), filipradenovic@yahoo.com (F. Radenović).

0165-1684/$ - see front matter © 2013 Elsevier B.V. All rights reserved.
http://dx.doi.org/10.1016/j.sigpro.2013.01.005

plane. Thus, it is easily removed by omitting, for each frequency, a fixed number of the highest STFT samples, as it is proposed in [15]. By summing the rest of the STFT values, over time, the FT of the rigid body is obtained. This approach is very simple to use and produces better results than the other approaches [9–14]. However, since the same number of the highest STFT samples is removed for each frequency, some of the STFT samples that correspond to the rigid body are removed by this procedure, as well. Influence of the missing STFT values to the concentration of the reconstructed rigid body is analysed analytically and by simulations in [15]. It has been shown that, after summing the remaining STFT values over time, there will be a highly concentrated component corresponding to the original Fourier transform (FT) (that would be obtained by summing all the STFT samples), surrounded by low-concentrated values (corresponding to the omitted STFT samples). Number of omitted rigid body samples in the STFT, that cause residual spreading in the reconstructed FT, is high. Therefore, classical optimization approaches cannot be used in their reconstruction due to the high computational load. In this paper, we propose a genetic algorithm for the estimation and recovering of the missing STFT samples that correspond to the rigid body.

Genetic algorithms are widely used as stochastic optimization methods [16–18]. They start with an initial population composed of a number of possible solutions (individuals represented by chromosomes). Then, by emulation of the evolutionary process in the nature, i.e. by crossover of individuals, where the best adopted individuals (those with the highest fitness) have the highest chance to survive and to be recombined with the others, and mutation, different populations of fixed size are generated. After a couple of generations, the average fitness of the new populations increases, meaning that they consist of the best adopted individuals from each generation and their recombinations. In our application, as the final solution we use the best adopted individual of the last generation, i.e. the one with the highest fitness.

Chromosomes of each individual consist of potential phase values of the missing STFT samples that correspond to the rigid body. The number and positions of these samples in the TF plane can be easily determined. We know that Hann(ing) window is used for the STFT calculation and zero-padded in order to produce the same number of samples as in the FT [15]. Therefore, we know the width (the number of columns) of the STFT that corresponds to the rigid body. The position of the rigid body is obtained from the position of the peak in the FT reconstructed by summing the STFT samples remaining after the m-D removal. On the other hand, for each time instant (row), the STFT samples of the rigid body are equal to the low concentrated FT of the used window, shifted to the frequency of the rigid body. Then, for each frequency (column), the STFT samples of the rigid body are with equal amplitudes, but with different phases, except at the position of the rigid body, where they are in phase [15]. Therefore, the amplitudes of the missing STFT values at the same frequency (column) can be set to the median of the amplitudes of the remaining STFT values at that frequency. We only need to estimate their phases. The initial population is formed by randomly choosing values of the phases within $[0,2\pi)$ for each individual. Possible solutions are then binary coded, and they form chromosomes of an individual. In each generation, the new individuals are generated by uniform cross-over, after selecting two individuals which will exchange their genetic material, [18]. The individuals that are better adopted (with higher fitness) will be selected with higher probability. In [15], it has been shown that after summation of the STFT samples over time, the obtained FT of the rigid body is the same as its FT directly calculated with a window close to the rectangular one (with a small transition at the ending points) or even with the rectangular window. Thus, the FT of the rigid body component reconstructed by summing over time the STFT samples filled with the recovered values should have only one non-zero value, at the frequency that corresponds to its position. Consequently, for the fitness calculation of an individual, the sum of the absolute squared values of the corresponding reconstructed FT, except the maximal one, is calculated for the frequencies covered by the STFT of the rigid body. The individual with the smallest sum (i.e. the smallest residual spreading) has the highest fitness, and represents the best phases estimation of the missing STFT samples.

The paper is organized in five sections. In Section 2, the radar signal model and the procedure for the rigid body separation, based on the L-statistics, are presented. The genetic algorithm for the reconstruction of the missing STFT samples is proposed in Section 3. Calculation complexity of the proposed algorithm is also discussed in this section. Performance of the proposed method is illustrated through simulations in Section 4, while the conclusion is given in Section 5.

2. Rigid body separation based on the L-statistics

Consider a continuous wave (CW) radar that transmits signal in a form of coherent series of M chirps [19]. The received signal, reflected from a target, is delayed with respect to the transmitted signal for $t_d = 2d(t)/c$, where $d(t)$ is the target distance from the radar and c is the speed of light. This signal is demodulated to the baseband, with possible distance compensation and other preprocessing operations (such as pulse compression) [19,20]. In order to analyze the influence of cross-range non-stationarities in the radar imaging, we will consider only the Doppler part in the received signal of a point target, in the continuous dwell time, as it is usually done in the radar literature [19]:

$$s(t) = \sigma e^{j2d(t)\omega_0/c}, \tag{1}$$

where σ is the reflection coefficient of the target, while ω_0 is the radar operating frequency. The repetition time of a single chirp will be denoted by T_r, while the number of samples within each chirp is N. The CIT is $T_c = MT_r$.

The Doppler part of the received radar signal that corresponds to a rigid body point can be modelled as a complex sinusoid, while the Doppler part that corresponds to a rotating reflector is sinusoidally frequency

modulated (FM) signal [15]. In general, for an arbitrary m-D motion, it is an arbitrary FM signal. Detail derivation of this model is given in [15]. The received signal, for a system of point scatterers, can be modeled as a sum of individual point scatterer responses [19]. Radar signal for K rigid body points and P fast moving m-D points can be written as [15]

$$s(m) \cong \sum_{i=1}^{K} \sigma_{Bi} e^{jy_{Bi}m} + \sum_{i=1}^{P} \sigma_{Ri} e^{jA_{Ri}\sin(\omega_{Ri}m+\varphi_i)}, \quad (2)$$

where σ_{Bi} and σ_{Ri} are reflection coefficients of the rigid body reflector and rotating reflector, respectively, y_{Bi} is proportional to the position of the rigid body reflector, A_{Ri} is proportional to the distance from the rotating reflector to the center of rotation, while ω_{Ri} is proportional to its rotating rate, $m=0\ldots M-1$. Sinusoidal FM signal is analyzed as a model of the m-D that appears as a result of rotation or vibration of object's reflectors since it is quite common form of the m-D. Also, its analytical form can be easily obtained, so it is nice for qualitative analysis [15]. The m-D removal approach proposed in [15] works well not only for the rotation caused m-D, but also for any arbitrary fast moving m-D point with $\sigma_{Ri}e^{jf_i(m)}$, where $f_i(m)$ is an arbitrary highly non-linear function of the m-D point motion.

The frequency content of the rigid body is constant over time, and for its representation, it is enough to use the FT. However, the frequency content of the rotating reflector is time dependent and the FT is not an adequate tool for its representation. The simplest way to localize the signal behavior in shorter intervals, within the CIT, is by applying a window function to the standard FT. The resulting short-time Fourier transform is defined in discrete form as

$$STFT(m,k) = \sum_{i=0}^{M-1} s(i)w(i-m)e^{-j2\pi ik/M}, \quad (3)$$

where $w(i)$ is a window function used to truncate the considered signal. The window width is M_w, $w(i)\neq 0$ for $-M_w/2 \le i \le M_w/2-1$, and it is zero-padded up to M, the same number of samples as the FT of the original signal would have. In this way, we have the same STFT's frequency grid as in the FT, so that the FT can be reconstructed from it, without interpolation, with the concentration close or equal to the concentration of the original FT. The concentration could be restored to the original one by summing all low concentrated STFT (complex) values over m. Since we calculated $STFT(m,k)$ with the window of the width M_w, there are two possibilities for its summation: (a) For all time instants $0 \le m \le M-1$, when the signal $s(i)$ has to be zero-padded for $-M_w/2 \le i < 0$ and $M \le i < M+M_w/2-1$; (b) For instants $M_w/2 \le m \le M-M_w/2$, when zero-padding of $s(i)$ is not used. Reconstruction formula, for the case with zero-padding is

$$\sum_{m=0}^{M-1} STFT(m,k) = \sum_{i=0}^{M-1} s(i)\left[\sum_{m=0}^{M-1} w(i-m)\right] e^{-j2\pi ik/M} = \sum_{i=0}^{M-1} s(i)w_1(i)e^{-j2\pi ik/M} = S_{w_1}(k). \quad (4)$$

In the case when the STFT is calculated for each time instant (time step one in the STFT calculation), the resulting window $w_1(i)$ is constant, $w_1(i)=const$, for $0 \le i \le M-1$, for any used window. Then, the pure rectangular window $w_1(i)$ will be obtained, for any window $w(i)$. It means that we will be able to reconstruct the FT with a concentration equal to the one in the original FT, by using low concentrated STFTs, calculated with narrow windows. In this way, we will restore the high concentrated radar image, although we used low concentrated STFT in the analysis. The analysis is not restricted to the step one in the STFT calculation. The same resulting window would be obtained for a step equal to a half of the window width ($M_w/2$) and a Hann(ing), Hamming, triangular or rectangular window. The same stands for steps equal to $M_w/4$, $M_w/8$, etc.

The presented mechanism of restoring the original concentration of the FT, in the conjunction with the knowledge of the TF patterns behavior of the fast moving and rigid scattering points, led us to an algorithm for the m-D free, highly concentrated, radar image [15]. The rigid body and the fast moving points behave differently in the TF representation of the returned radar signal, within the CIT. In Fig. 1(a) the STFT of one rigid body reflector and one fast rotating reflector modeled as (2), with $K=1$, and $P=1$, is presented. The rigid body signal is almost constant in time (stationary), while the fast-varying m-D part of the signal is highly non-stationary. This part of the signal keeps changing its position in the frequency direction.

The basic idea for separating the rigid body and the fast rotating part is in sorting the STFT values of the returned radar signal along the time axis, within the CIT, Fig. 1(b). Since the rigid body return is stationary, the sorting procedure will not significantly change the

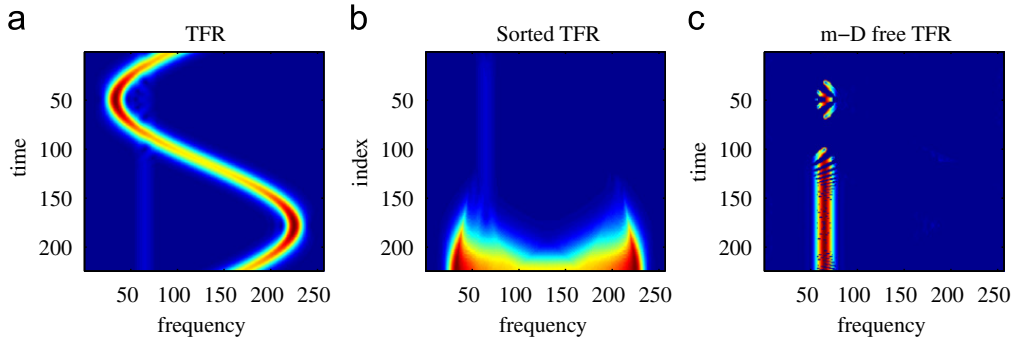

Fig. 1. One rigid body reflector and one fast rotating reflector: (a) STFT; (b) sorted STFT; (c) STFT after m-D removal.

distribution of its values. However, the fast-varying m-D part of the signal is highly non-stationary. It exists, for each frequency, over a wide range of frequencies, in short time intervals. Thus, after sorting the STFT along the time axis, the m-D part of the signal has strong values at the wide frequency range, but for a few samples only. By removing, for each frequency, several strongest values of the sorted STFT, we will eliminate most or all of the m-D part of the signal. After this removal in the sorted plane, the remaining samples are repositioned at their original positions, Fig. 1(c). We will get the reconstructed rigid body radar image by summing the remaining STFT values over time (in the sorted or in the repositioned domain).

Let us consider a set of M (or $M-M_w$ if the signal is not zero-padded) elements of the STFT, for a given frequency k:

$$\mathbf{S}_k(m)=\{STFT(m,k), m=0,1,\ldots,M-1\}.$$

After sorting $\mathbf{S}_k(m)$ along the time, for a given frequency k, we obtain a new ordered set of elements $\Psi_k(m)\in\mathbf{S}_k(m)$ such that $|\Psi_k(0)|\le|\Psi_k(1)|\le\cdots\le|\Psi_k(M-1)|$. Of course, addition is a commutative operation, so if we use the whole set, we will get

$$\sum_{m=0}^{M-1} STFT(m,k)=\sum_{m=0}^{M-1}\Psi_k(m)=S_{w_1}(k). \tag{5}$$

In the L-statistics form of this summation we will, for each k, omit $M-M_Q$ of the highest values of $\mathbf{\Psi}_k(m)$ and produce the L-estimate of $S_{w_1}(k)$, denoted by $S_L(k)$, as

$$S_L(k)=\sum_{m=0}^{M_Q-1}\Psi_k(m), \tag{6}$$

where $M_Q=\mathrm{int}[M(1-Q/100)]$ and Q is the percent of omitted values.

Since we have eliminated some of the TF representation (TFR) values, we will analyze the influence of incomplete sum in (5). This is the same theory like the L-statistics theory applied to the noisy or non-noisy data [21].

Assume that only points in $m\in D_k$ are used in summation:

$$S_L(k)=\sum_{m\in D_k} STFT(m,k), \tag{7}$$

where, for each k, D_k is a subset of $\{0,1,2,\ldots,M-1\}$ with M_Q elements. Within the framework of the previous analysis, it means that there will be a highly concentrated component $S_{w_1}(k)$ surrounded by several low-concentrated values $\sum_{m\notin D_k} STFT(m,k)$. Note that the amplitude of $STFT(m,k)$ is M times lower than the amplitude $S_{w_1}(k)$, since $S_{w_1}(k)$ is obtained as a sum of M values of the STFT. In general, by removing lets say $(M-M_Q)$ values in m, we would get one very highly concentrated pulse, as in $S_{w_1}(k)$, and $(M-M_Q)$ low-concentrated components of the type $STFT(m,k)$, being spread around the peak of $S_{w_1}(k)$ and summed up by different random phases. Only the peak value is summed in phase. Consider, in the STFT of the rigid body only, where $W(k)$ is the discrete FT (DFT) of the used window:

1. Case for $k=k_0$ corresponding to the position of the rigid body point: At this frequency, all terms in the sum are the same and equal to $W(0)$. Thus, the value of $S_L(k)$ does not depend on the positions of the removed samples. Its value is $S_L(k_0)=M_Q W(0)$.
2. Case for $k=l+k_0$, where $l\neq 0$: Removed terms in (5) are of the form $x_l(m)=W(l)e^{j2\pi ml/M}$. They assume values from the set $\Phi_l=\{W(l)e^{j2\pi ml/M},\ m=0,1,2,\ldots,M-1\}$, with equal probability, for a given l.

In [15], two possible approaches to establish Q are presented: to use a constant value of Q or to adaptively calculate this value based on the L-statistics. However, it is suggested that the simplest way to use the procedure for the m-D removal is to apply it with a constant threshold, for example $Q=50\%$. In this way the m-D would be removed, while the rigid body would not be much degraded. Moreover, we will benefit in the case of impulse noise, since we will avoid the highest values, which are most influenced by a noise. Removing the highest values of the STFT induces benefit in the case of close rigid body reflectors, as well. By the proposed method, high signal resolution may be achieved even in the case when the separation is not possible in the original FT over the whole CIT [15]. Bearing all this in mind, we have mostly removed 50% of the highest STFT values, as it is done in [15].

By the explained procedure, the m-D free STFT is obtained, but missing values of the rigid body induce residual smearing around the peak in the FT reconstructed by using the remaining STFT samples. Residual smearing may be avoided by recovering the omitted STFT values that correspond to the rigid body. The number of these samples is high, as it will be shown in the next section. Thus, it would be difficult to apply any classical optimization procedure. They would induce multidimensional search. Therefore, we need some alternative solution, such as using a genetic algorithm.

3. Genetic algorithm for the missing STFT values estimation

Genetic algorithms are stochastic methods that are widely used for the optimisation procedure [16–18], especially when the searching procedure should be performed over multi-dimensional space. Although they are applied in a wide range of areas, all of them consist of the same components.

The first issue that should be resolved in a genetic algorithm is how to represent possible solutions, i.e. to define chromosomal representation of individuals in a population. Each individual represents possible solution coded in a certain way. The binary codes for chromosomal representation are well adopted, since they have the minimal alphabet, as it is recommended by Holland [22].

By knowing the form of the STFT of the rigid body, it is easy to decide how to represent the possible values of the missing STFT samples. In the previous section and in [15], it is shown that all the STFT values at the frequency that corresponds to the frequency of the rigid body component $(k=k_0)$ are equal to $W(0)$. Thus, for this frequency (column in the STFT if we consider the STFT as matrix), we do not have to estimate values of the missing samples, and we fill them up with the median of the remained STFT

samples at this frequency. On the other hand, for $k=l+k_0$, where $l\neq 0$, the removed STFT samples are of the form $x_l(m)=W(l)e^{j2\pi ml/M}$, and we know that they assume values from the set $\Phi_l=\{W(l)e^{j2\pi ml/M},\ m=0,1,2,\ldots,M-1\}$, with equal probability, for a given l. Their absolute values are equal to $W(l)$, while they have different phases. Therefore, for each frequency, close to k_0, we calculate amplitudes of the missing STFT samples as median of the amplitudes of the remaining STFT samples in the corresponding column (frequency), while their phases are randomly chosen from the set $[0,2\pi)$ and binary coded. The obtained combination of possible phases for the missing STFT samples makes chromosomal representation of one individual in the initial population.

For the reconstruction of the rigid body FT it is enough to estimate, for each time instant, only non-zero STFT values of the corresponding STFT representation of the rigid body. We work with the DFT and we know that, for each time instant, the STFT of the rigid body corresponds to the FT of the used Hann(ing) window, centered at k_0. We know that the DFT of the Hann(ing) window is consisted of only three non-zero values. However, since we zero-padded the window up to M, in order to obtain the same frequency grid as in the original FT, we have additional non-zero STFT values. The number of these non-zero values can be easily calculated as

$$|l|\leq 1+2(M/M_w-1). \tag{8}$$

On the each side of k_0 we have the initial non-zero value, while as a consequence of zero-padding, we will have M/M_w-1 non-zero STFT samples between zero and this initial value, as well as between this value and non-zero value at $k=k_0$. The position of rigid body $k=k_0$ can be determined as the position of maximum in the reconstructed FT. Thus, we know exactly the number and positions of the missing STFT values that correspond to the rigid body. Note that, although some non-zero values that correspond to the side lobes of the FT of the Hann(ing) window will appear as a consequence of zero-padding, they are very small, and we do not take them into consideration. If we would remove, for example, 50% of STFT samples, i.e. $M_Q=M/2$, the length of each individual would be

$$L_{ch}=2[1+2(M/M_w-1)]M/2\cdot 3,$$

where each phase is coded with three bits. Although this may seem to be very long chromosomal representation, the algorithm performs very fast, since the encoding/decoding procedure is simple. Each three bits represent a phase obtained as their decade value multiplied by $2\pi/8$.

The second task that should be resolved in a genetic algorithm is how to create an initial population. There are at least three approaches. The first one is to randomly select values from a set of possible solutions, than one can use some priory knowledge related to a considered problem or select them deterministically in order to keep equal distance between two chromosomes. In our application, the first approach is used.

The third task is to find proper function for "quality" evaluation of individuals (fitness function). The fitness function is directly related to the problem that should be solved. In our application, we know that, if all the STFT samples were to be summed, $S_{w_1}(k)$ would be obtained, as in (4). In the previous section we showed that this is the FT of the original signal calculated with the normalized resulting window $w_1(i)$ which is the rectangular one (or, without zero-padding, the window close to the rectangular one, with a small transition at the ending M_w points). If we use the rectangular window (no window), the DFT of the rigid body would have only one non-zero value at the position k_0. Thus, for the quality (fitness) evaluation of an individual, we fill the phases of the missing STFT samples by their decoded values, reconstruct the FT by summing the obtained STFT, and calculate its energy for $k=k_0\pm l$, where $l\neq 0$, and $l\leq 1+2(M/M_w-1)$ [23]:

$$E=\sum_{\substack{|l|\leq 1+2(M/M_w-1)\\ l\neq 0}}\left|S_{w_1}(k_0+l)\right|^2. \tag{9}$$

The amplitudes of the missing STFT samples are estimated as the median of the remaining STFT samples at the same frequency. The individual with the lower energy (9) has the higher fitness (it is closer to the optimal solution – reconstructed FT as a peak at k_0 surrounded by the zero values).

When we have fitness function, we can perform the selection of individuals for the recombination. Like in nature, the individuals better fitted to the environment have a higher probability to recombine their genetic material with the other individuals and to survive to the next generation. Effective selection of the parents can be done in many ways: tournament, proportionate selection, etc. [18]. Tournament selection, consisted of tournaments between a fixed number of randomly selected individuals, is used in our realisation of genetic algorithm. Individual with the highest fitness is the winner of the tournament, and it is chosen for the recombination. The effectivity of this selection may be easily adjusted by changing only one parameter – the tournament size. In our realisation 1/5 of the entire population participate in a tournament, while the number of tournaments is selected in order to potentially produce the same number of individuals as in the current population. We said potentially because, after selection of the parents, cross-over (recombination of genes) is performed with some predefined probability. The probability of cross-over is high, usually between 0.5 and 0.9. Cross-over probability of 0.7 is used in our realisation. Uniform cross-over scheme is also used. For each gene one of two parents is randomly selected and its gene is taken for the first child, while the gene at the same position is taken from the other parent for the second child. The procedure is repeated until two children are formed. Mutation (inversion of randomly selected genes) is then used in order to prevent convergence toward non-optimal solution (for example local extremum). Nevertheless, if mutation is performed with high probability, it may slow down the convergence of the algorithm. Since we have long chromosomes, we performed the mutation of one bit in each fifty bits with the probability of 0.25.

After the recombination is finished, it must be decided which individuals will form the new generation. In our

realisation, the old and new generation are put together and those with the best fitness function are chosen, so that the fixed size of generation is kept. One hundred individuals per generation are used.

The explained procedure is repeated for a fixed number of generations or until some predefined condition is met. In our realisation the algorithm may last for 100 generations, or until in five subsequent generations the highest fitness remains unchanged. The second condition was first met in all of our simulations, after approximately 76 generations. Decoded values of phases represented by the chromosomes of an individual with the highest fitness are taken as the phases estimation of the missing STFT samples.

The proposed algorithm may be used for the reconstruction of the missing values in the case when we have more than one rigid body reflector. For determining the number and positions of the rigid body's reflectors, from the reconstructed m-D free FT, we have used a thresholding procedure, similar to the one used in [24]. The analysed signal is actually the radar signal for a range cell in which a target is detected. A procedure for detection of ranges in which there is a target is proposed in [24] and it can be easily performed by setting the adequate threshold. Therefore, at the beginning of this modified procedure, we may assume that there is at least one rigid body reflector in the examined signal and threshold ε'' is set as 2% of the energy of the m-D free signal. The position of the rigid body reflector (maximum) in the m-D free FT is determined and it is removed by setting zeros at the position of the maximum and surrounding l samples (8). Then, the remaining energy is calculated. While the remaining energy is higher than the threshold ε'' the number of rigid body reflectors is incremented and the procedure of finding their positions and removing them from the signal is repeated. In the considered radar applications, this threshold selection procedure produced accurate results. Higher values for ε'' than in [24] are used here, since the reconstructed FT was not completely concentrated, as a result of the missing STFT samples, and we wanted to avoid a possibility of false rigid body detection.

3.1. Summarised procedure for the rigid body reconstruction after m-D removal

The proposed procedure for counting the number of rigid body reflectors and reconstruction of their missing STFT values can be presented by the following steps:

Step 1. Remove, for each frequency, a fixed number (usually 50%) of the highest STFT values and sum the rest along the time to obtain the m-D free FT $S_L(k)$ (7). Set the threshold ε'' as 2% of the energy of the m-D free signal and calculate the width of a rigid body reflector by using (8). Initialize the number of rigid body reflectors as $kk=1$. Find and remember the position of the rigid body reflector (maximum of the $S_L(k)$) and remove it by setting zeros at its position and at the neighboring l samples on its each side.

Step 2. While the remaining energy is higher than the threshold ε'', increase the number of rigid body reflectors $kk=kk+1$. Calculate and remember the position of the rigid body reflector and remove it by setting zeros at its position and at the neighboring l samples on its each side.

Step 3. If $kk>0$, estimate the amplitudes of the rigid body's STFT samples, removed in the first step, as the median of the remaining STFT amplitudes at the same frequency. Take that the rigid body reflector has non-zero values at l frequencies on each side of its position. Form an initial population of the genetic algorithm (100 individuals), where each individual represents phases of the non-zero missing rigid body's STFT samples. Choose each phase value randomly from the set $[0,2\pi)$ and code it binary. Calculate the fitness of each individual as (9), where the chromosomal representation of an individual is taken as the phases estimation of the missing STFT samples of the rigid body reflector and S_{w_1} is recovered as (4).

Step 4. For 100 generations or until the highest fitness remains unchanged in five subsequent generations, select individuals for the recombination by using tournaments. Perform uniform cross-over on the winners of the tournaments, with probability of 0.7. Perform mutation of the obtained children with probability of 0.25. Put the new individuals and the old ones together. Calculate the fitness of each new individual as (9), where the chromosomal representation of an individual is taken as the phases estimation of the missing STFT samples of the rigid body and S_{w_1} is recovered as (4). Take 100 individuals with the highest fitness as the new generation.

Step 5. From the last generation, take the individual with the highest fitness as the final estimation of the phases of the non-zero missing rigid body's STFT samples. Sum the recovered STFT over the time and take the obtained FT as the final estimation of S_{w_1} for that rigid body reflector. Decrease the number of the rigid body reflectors $kk=kk-1$ and go to Step 3.

In the radar image, these steps should be applied for the range cells in which a target is detected, by the procedure given in [24].

3.2. Calculation complexity of the genetic algorithm

Genetic algorithm is a stochastic process so precise analytic expression for its calculation complexity cannot be given. Its calculation complexity depends on the initial generation, cross-over, mutation, etc. However, calculation complexity for a genetic algorithm with fixed populations' size is usually measured by the number of fitness function evaluations during its run [25]. The number of fitness function evaluations can be calculated as product of population size and number of generations. The precise number

of generations cannot be given for genetic algorithm. Our genetic algorithm may run for 100 generations, or until in five subsequent generations the highest fitness remains unchanged. We have rerun our algorithm over 200 times for the signal composed of one rigid body and one m-D point, presented in Fig. 1 and the first example. In each run the second condition was first met. Maximal number of generations was 90, minimal number was 63, while the mean number was 76. The mean duration of its realization on Intel i3 processor 2.3 GHz was 33.0102 s. Although the precise number of the populations cannot be given, the worst case analysis can be done, i.e. 100 of generations can be used for the evaluation of the calculation complexity. We use 100 of individuals per generation leading to [100 × 100] fitness function evaluations in the worst case.

If we tried to estimate the missing STFT's values by using the standard optimisation techniques, multidimensional search procedure should be performed. We may use the same optimization function here as in the genetic algorithm. Our goal would be to find a combination of the phases for the missing STFT samples for which we have the smallest energy of the samples around rigid body peak in the reconstructed FT. If the same set of possible values for the phases, as in the genetic algorithm, were to be used, we would have eight possible values of phase for the each STFT sample. In addition, since we usually remove 50% of samples, then for the rigid body reflectors we will remove $M/2$ samples. For K rigid body reflectors we remove approximately $K2[1+2(M/Mw-1)]M/2$ samples in total. For example, for $K=5$, $M=256$ and $M_w=32$, if we calculate the STFT for each time instant then we remove about 19 200 samples. The number of fitness function evaluations would be $8^{19\,200}$ in this case, instead of $5\times 10\,000$ calculations by genetic algorithm. Even if we calculate the STFT only after each $M_w/4$ instants, the total number of rigid body samples in the STFT, that should be reconstructed, is very large.

3.3. Variance and convergence of the genetic algorithm

Although we use the genetic algorithm for the estimation of the STFT values of the rigid body that are rejected during the m-D removal procedure, the proposed algorithm is not completely stochastic, as the other genetic algorithms are. The position of the maximum that corresponds to the rigid body in the reconstructed m-D free FT and the width of the STFT of the rigid body are used as input arguments. Therefore, we a priori know the number of the missing STFT samples that should be recovered, and their positions. Then, we use the fact that the STFT samples of the rigid body are with the same amplitudes for each frequency, while they are with different phases, except at the frequency corresponding to the rigid body's position (peak) in the reconstructed FT, where they are in phase. Consequently, only the phases of the missing STFT samples are stochastic. However, our algorithm does not diverge in the sense of producing ghost rigid bodies. It will always give us rigid body at the same position as the one in the initial FT.

Theoretically, it may happen that the genetic algorithm based reconstructed FT is with lower concentration than the m-D free FT. Fitness function is measure of concentration of a FT. Therefore, we analysed probability of not convergence and variance of the fitness function. We assumed that our algorithm does not converge if the FT reconstructed by using the recovered STFT samples is with lower concentration than the initial m-D free FT. We have rerun the first example 200 times, and the theoretical divergence case has never happened. Divergence detection is on the other hand straightforward. We should compare the energy of the side lobes in the initial m-D free FT with the energy (fitness) of the side lobes in the FT reconstructed by using the proposed genetic algorithm. If the last one is higher, the genetic algorithm should be rerun. Note that only one additional calculation of fitness function is involved by adding divergence detection.

The variance of the best solution's fitness function, obtained for 200 reruns of the genetic algorithm for the signal composed of one rigid body and one m-D point, presented in Fig. 1 and the first example, is 4.6563×10^{-8}, mean value is 1.0004, standard deviation is 2.1579×10^{-4}, maximal value is 1.016. Fitness function of the initial m-D free FT is 1.7345. We can conclude that even the worst solution of the genetic algorithm is with significantly higher concentration than the initial m-D free FT.

4. Simulation study

Example 1. Radar return of one stationary reflector and one rotating reflector modeled as (2)

$$s(m)=e^{-j0.5\pi m}+15e^{j96\,\cos(2\pi m/256)} \tag{10}$$

is analysed in this example. The STFT of the resulting signal, calculated with the Hann(ing) window with $M_w=M/8$, is presented in Fig. 2(a). It can be seen clearly that the frequency content of the rotating reflector changes over time in a wide range of frequencies, and it partially covers the rigid body, which is constant. The original FT of the considered signal is presented in Fig. 2(d). The rigid body cannot be detected from the FT. It is completely masked by the m-D effect. Therefore, the procedure for the m-D removal is employed. The STFT samples remaining after removal of the m-D by the procedure proposed in [15], i.e. by rejecting (setting to zero), for each frequency, 50% of the highest STFT samples, are presented in Fig. 2(b). The m-D effect is removed, but a significant portion (50%) of the STFT samples that correspond to the rigid body are missing as well. The FT obtained by summing the remaining STFT samples over time is shown in Fig. 2(e). The obtained FT has one highly concentrated component that corresponds to the FT of the rigid body, which would be obtained by summing all of its STFT samples, surrounded by low-concentrated values, which are a consequence of the missing STFT samples of the rigid body. The position of the rigid body, needed for the proposed genetic algorithm, is determined as position of the maximum in this FT. The STFT obtained after recovering missing STFT samples by the proposed genetic algorithm is shown in Fig. 2(c). By summing over time the recovered STFT, the FT in Fig. 2(f) is obtained. The residual spread around the highly concentrated component is

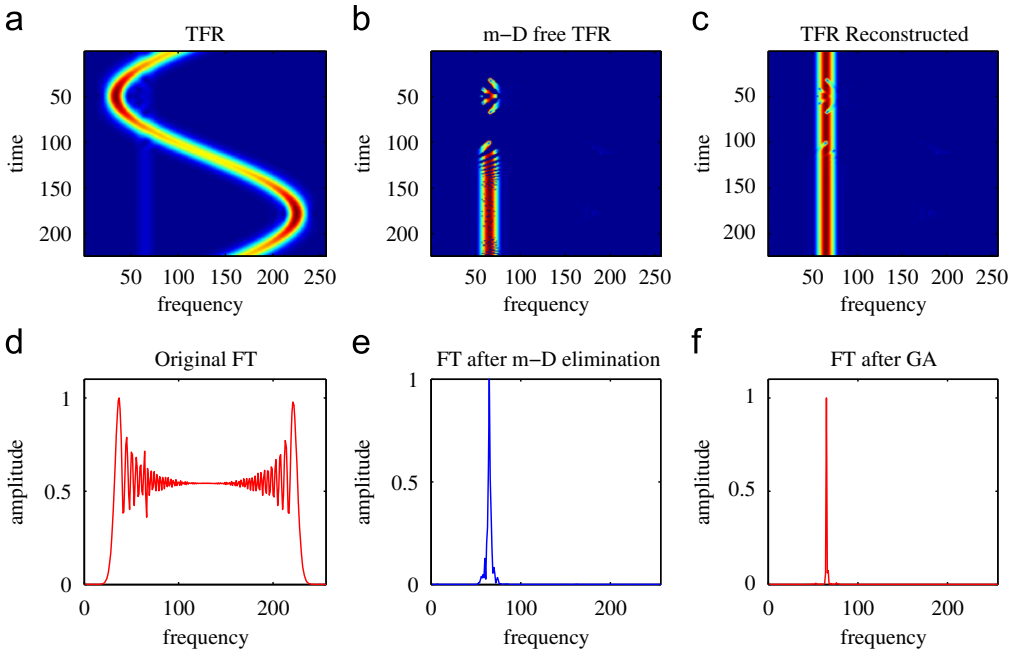

Fig. 2. Radar return of one stationary reflector and one reflector causing m-D: (a) STFT of the original signal; (b) STFT of the rigid body after m-D removal; (c) STFT of the rigid body after reconstruction by the proposed genetic algorithm; (d) FT of the original signal; (e) FT of the rigid body obtained by summing over time the STFT remained after the m-D removal; (f) FT of the rigid body obtained by summing over time the STFT reconstructed by the proposed genetic algorithm.

avoided, and the FT of the rigid body is obtained with almost the same concentration as it would have been if the m-D was not present at all.

Example 2. In [15], it has been shown that the proposed method for the m-D removal is robust to noise because it is L-statistics based. In order to test performances of our genetic algorithm in the presence of noise, we consider here the same signal as in the previous example, but in the presence of complex valued, white Gaussian noise with variance $\sigma^2 = 4.5$. The STFT of the original signal and its FT are presented in Fig. 3(a), (d), respectively. For the rigid body FT reconstruction we have summed over time, for each frequency, 50% of the smallest STFT values. The summed STFT samples and the corresponding FT are presented in Fig. 3(b), (e), respectively. The procedure for the m-D removal and the FT reconstruction is robust to noise. However, the missing STFT samples do influence the concentration of the reconstructed FT. Therefore, the proposed genetic algorithm is applied to recover the missing STFT samples of the rigid body. By using the STFT in which the missing samples are filled with the values estimated by the proposed genetic algorithm (Fig. 3(c)), instead of setting them to zero as in [15] (Fig. 3(b)), the concentration of recovered FT (Fig. 3(f)) is improved. The obtained FT is almost of the same concentration as it would have been if the m-D was not present in the first place.

Example 3. In this example the proposed method is tested on a signal

$$s(m) = \sum_{i=1}^{K} e^{jy_{Bi}m} + 5e^{j96\cos(2\pi m/256)},$$

with $K=5$ components of constant frequency (used to model the rigid body reflectors) and one sinusoidally FM component (used to model the rotating reflector) with: $y_{Bi} = [1.7\pi, 1.8\pi, 1.9\pi, 2\pi, 2.1\pi]$, for $i=1,2,3,4,5$, $M=256$ and $M_w = M/4$. M_w influences the concentration of the STFT. Higher M_w produces higher frequency concentration of the STFT, while concentration along time would be decreased. We use higher value of M_w in this example, than in the other examples, since we have multicomponent signal and we want to decrease the number of the STFT values that should be estimated. Namely, higher value of M_w gives us thinner STFT of the rigid body, see (8). The optimal value of M_w can be calculated by using the concentration measures, so that it may be signal dependent, as it is proposed in [23]. The STFT of this signal is shown in Fig. 4(a). The constant components, which correspond to the rigid body reflectors, are covered by the sinusoidally modulated pattern which represents the m-D effect of the rotating reflector. The m-D part of the corresponding signal is eliminated (see Fig. 4(b)) by removing 50% of the highest STFT values, for each frequency. The reconstructed FT, obtained by summing along time the rest of the STFT samples is shown in Fig. 4(e), while the original FT is presented in Fig. 4(d). All five reflectors are successfully recovered in the FT reconstructed by the procedure proposed in [15]. However, they are not represented as five sharp peaks; there is residual spread, resulting from the missing STFT samples.

The proposed genetic algorithm may be applied to the case of many rigid body reflectors. The number of reflectors and their positions are first determined by using the proposed thresholding procedure. In this example ε'' is set to 2% of the entire energy of the m-D free signal. This simple procedure produces correct number of reflectors. After finding the number and positions of reflectors, the genetic algorithm is applied five times; once per reflector.

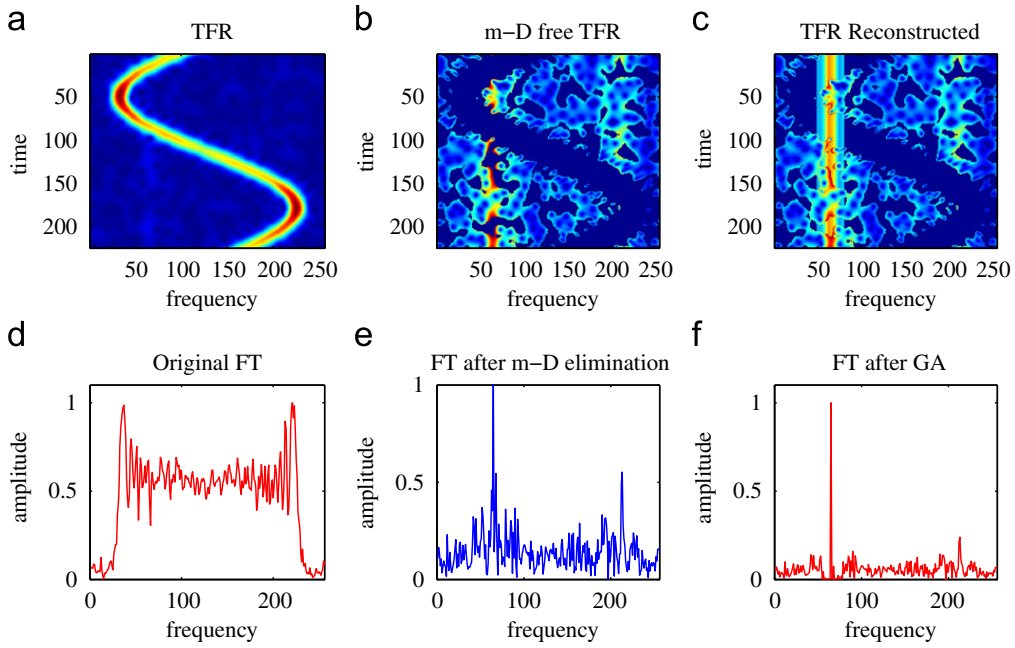

Fig. 3. Radar return of one stationary reflector and one reflector causing m-D in the presence of complex Gaussian noise with variance $\sigma^2 = 4.5$: (a) STFT of the original signal, (b) STFT of the rigid body after m-D removal, (c) STFT of the rigid body after reconstruction by the proposed genetic algorithm, (d) FT of the original signal, (e) FT of the rigid body obtained by summing over time the STFT remained after the m-D removal, (f) FT of the rigid body obtained by summing over time the STFT reconstructed by the proposed genetic algorithm.

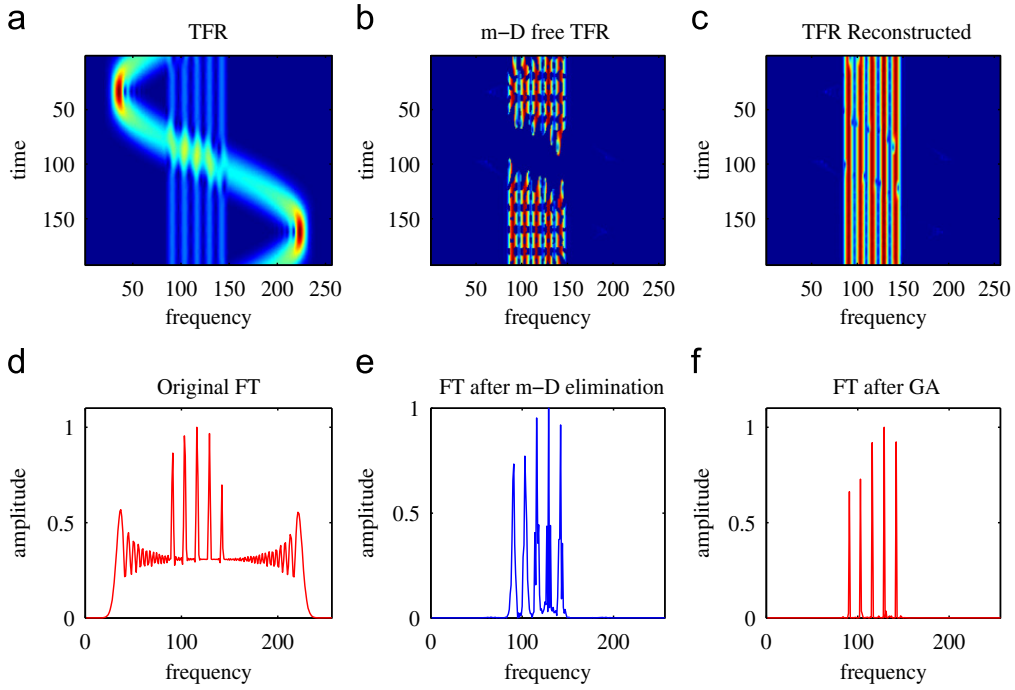

Fig. 4. Radar return of five stationary reflectors and one reflector causing m-D: (a) STFT of the original signal, (b) STFT of the rigid body reflectors after m-D removal, (c) STFT of the rigid body reflectors after recursive reconstruction by the proposed genetic algorithm, (d) FT of the original signal, (e) FT of the rigid body reflectors obtained by summing over time the STFT remained after m-D removal, (f) FT of the rigid body reflectors obtained by summing over time the STFT reconstructed by the proposed genetic algorithm. In one call of genetic algorithm one rigid body is reconstructed.

The STFT filled with the estimated values, for each rigid body reflector, is presented in Fig. 4(c), while the corresponding FT, obtained by summing over time the recovered STFT, is presented in Fig. 4(f). The proposed peak pealing procedure for counting the number of reflectors and genetic algorithm, called in the recursive manner, successfully reconstruct the missing STFT samples, and produce highly concentrated FT, even in the case of several rigid body reflectors.

Example 4. In [15], it has been shown that the proposed procedure for the m-D removal may be modified in order to deal with the uncompensated rigid bodies' motion. The case when the whole body of a target accelerates is

examined. The received radar signal, which corresponds to an accelerating target in the ISAR/SAR systems, is modeled as a linear FM [19]. In this example, three rigid body reflectors are simulated as three linear FM components with the same chirp-rate α, since the entire body performs the same motion. Moreover, in order to show that our algorithm will reconstruct the TFR values in a general case of the m-D, a more complex form of the m-D is used in this simulation, as in [15].

The STFT of the analysed signal, calculated with the Hann(ing) window with $M_w = M/8$, is presented in Fig. 5(a). The STFT of the rigid body is not constant during the time, as a result of its acceleration. Therefore, after sorting it, it is difficult to separate the rigid body from the m-D, Fig. 5(b). After summing $M/3$ the lowest STFT samples Fig. 5(b), the rigid body reconstruction like in Fig. 5(d) is obtained. The m-D is removed, but a significant part of the rigid body is as well removed. Rigid body reflectors are still invisible even in this reconstructed FT. Moreover, it is not convenient to use the FT for the representation of a rigid body with uncompensated acceleration.

Motion compensation prior to the procedure for the m-D removal is proposed in [15]. The linear frequency modulation of the rigid body's part, induced by its acceleration, is removed by dechirping the radar signal using an estimated chirp rate $\hat{\alpha}$. The main task was to estimate chirp-rate α. However, it is known that it can take values from the set $\Lambda = [-\alpha_{\max}, \alpha_{\max}]$, where $\alpha_{\max}$ is the chirp-rate that corresponds to the maximal expected acceleration (positive or negative). Then, parameter $\hat{\alpha}$ was estimated as the value from the set Λ for which we obtained the highest concentration of the reconstructed FT based on the STFT of the signal compensated for α and L-statistics. This reconstructed compensated FT was denoted by $S_{L,\alpha}(k)$, while its concentration was calculated as [23]

$$H(\alpha) = \left(\sum_{k=0}^{M-1} |S_{L,\alpha}(k)| \right)^2 \Big/ \sum_{k=0}^{M-1} |S_{L,\alpha}(k)|^2. \tag{11}$$

In this example, the same procedure as in [15], with $\Lambda = [-2 : 0.25 : 2]$ is used. The STFT of the signal dechirped by using the estimated optimal value $\hat{\alpha} = 1.25$, is shown in Fig. 5(e). After dechirping, rigid body reflectors are depicted as components with constant frequency in the STFT. These components are clearly visible in the sorted STFT, Fig. 5(f). By summing over time, for each frequency, $M/3$ of the lowest STFT samples we have reconstructed the FT of the rigid body, as it is presented in Fig. 5(h). In [15], it has been shown that the procedure is not too sensitive to $\hat{\alpha}$. Quite good results

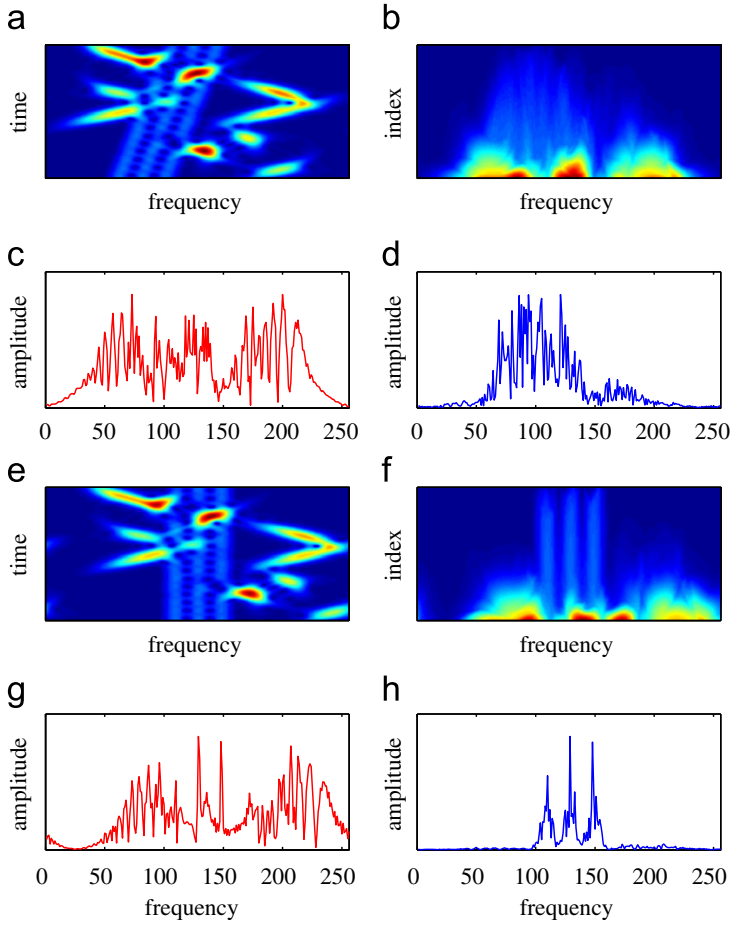

Fig. 5. Accelerating rigid body with a complex form of the m-D: (a) TFR of the signal without motion compensation, (b) sorted TFR of the original signal, (c) original FT of the analysed signal, (d) reconstructed FT of the accelerating rigid body without motion compensation, (e) TFR of the signal after motion compensation, (f) sorted TFR of acceleration compensated signal, (g) the FT of the original signal with motion compensation, (h) reconstructed FT of the accelerating rigid body with motion compensation.

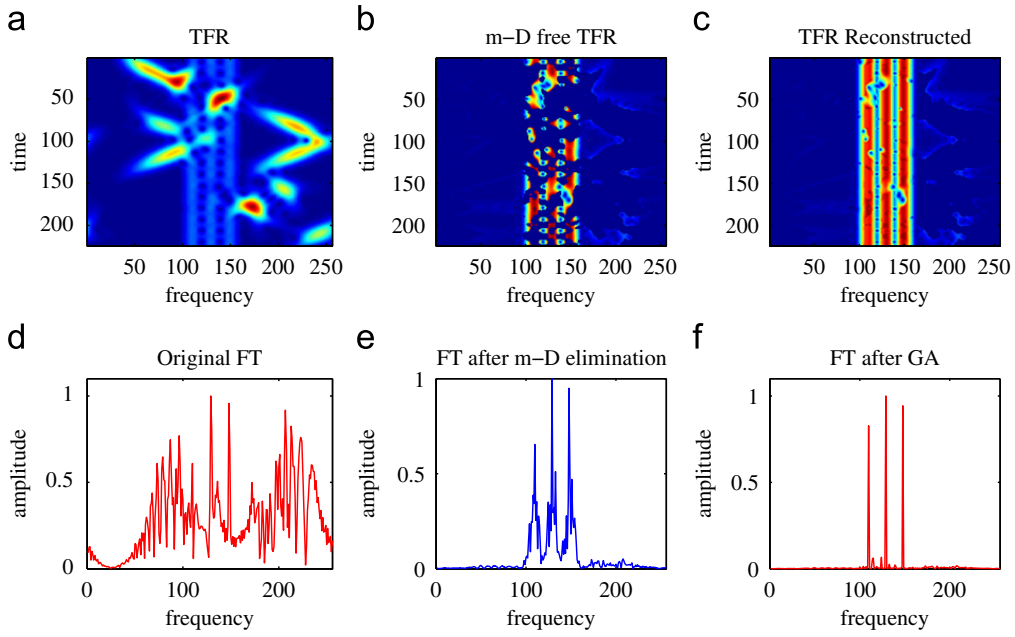

Fig. 6. Accelerating rigid body with a complex form of the m-D after motion compensation is performed on the signal: (a) STFT of the signal with motion compensation, (b) STFT of the rigid body after m-D removal, (c) STFT of the rigid body after recursive reconstruction by the proposed genetic algorithm, (d) FT of the signal with the motion compensation, (e) FT of the rigid body obtained by summing over time the STFT remained after m-D removal, (f) FT of the rigid body obtained by summing over time the STFT of three reflectors reconstructed by recursive call of the proposed genetic algorithm. In one call of genetic algorithm one rigid body's reflector is reconstructed.

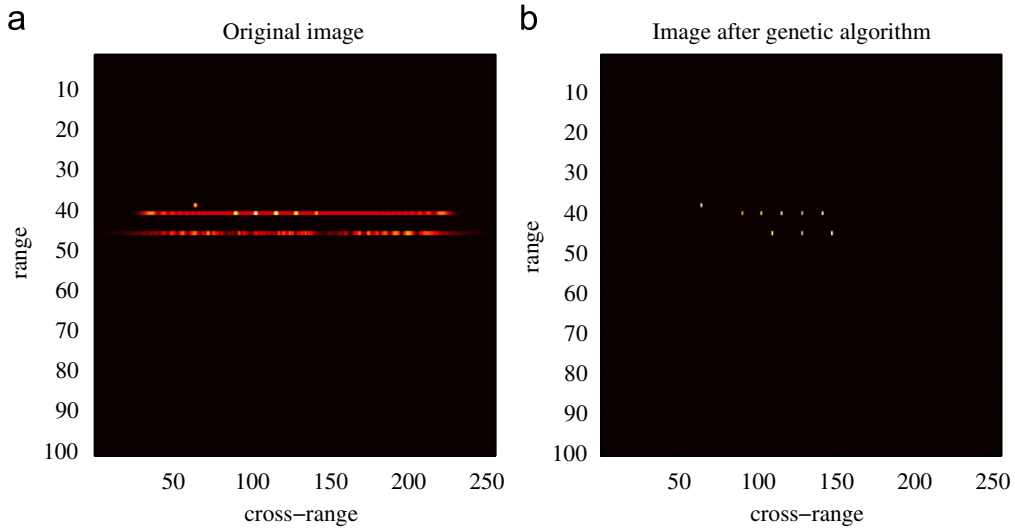

Fig. 7. Radar image of a target composed of the reflectors analysed in the previous examples: (a) original radar image and (b) radar image reconstructed after GA based estimation of the missing STFT samples.

were obtained with the neighboring values. With this example we would like to show that our algorithm works in the case of complex form of the very strong m-D. In order to completely remove the strong m-D, a higher number of the STFT samples in comparison to the other examples is removed, and the FT is reconstructed based on the remaining $M/3$ samples.

By the modification proposed in [15], we managed to remove the m-D and to reconstruct the FT of the rigid body, with the concentration high enough to detect its three reflectors. However, the concentration of the obtained FT could be significantly improved. In order to do so, the proposed procedure for counting the number and positions of the rigid body reflectors from the reconstructed FT (Fig. 6(e)) is used. The proposed genetic algorithm for the reconstruction of the missing STFT samples of dechirped m-D free signal, Fig. 6(b), is then applied for each reflector. The obtained STFT with the reconstructed missing samples of each reflector is presented in Fig. 6(c), while the FT reconstructed by summing its values over time is presented in Fig. 6(f). Concentration of this FT is significantly increased comparing to the concentration of the FT presented in Fig. 6(e). The FT with concentration almost as high as it would have been if there was no m-D, and without rigid body acceleration, is obtained. This example shows that the

performance of our algorithm does not depend on the type of m-D and rigid body motion.

Example 5. Signals presented in each of the previous examples may be considered as signals that correspond to a range bin in a radar image. Corresponding radar image, where reflectors from the first example are in 38th range bin, reflectors from the third example in 40th range bin, and reflectors from the fourth example in 45th, is shown in Fig. 7. The original radar image is presented in Fig. 7(a). From this image it is even difficult to determine the number of the rigid body reflectors. They are almost completely covered by the m-D. Radar image obtained (for the ranges of interest) by summing over time the m-D free STFT recovered by the proposed genetic algorithm (as it is shown in the previous examples) is presented in Fig. 7(b). All rigid body reflectors are recovered and well focused.

5. Conclusion

The micro-Doppler effect appears in the ISAR/SAR images in the case when there are fast moving reflectors in the observed scene. The m-D can severely decrease the quality and readability of the obtained radar image. Its detection and removal are very important for obtaining a focused image of the rigid body. An efficient algorithm for the m-D removal and reconstruction of the rigid body image, based on the L-statistics, exists. By removing the m-D components, this algorithm removes a part of the rigid body as well. In this paper we present a genetic algorithm to reconstruct the missing rigid body values. By simulated examples, it has been shown that this algorithm efficiently deals with residual spread in the rigid body components, making them almost as if m-D did not exist at all in the radar image.

References

[1] V.C. Chen, F. Li, S.-S. Ho, H. Wechsler, Analysis of micro-Doppler signatures, IEE Proceedings Radar, Sonar and Navigation 150 (August (4)) (2003) 271–276.

[2] V.C. Chen, Micro-Doppler effect in radar: Part I: phenomenon, physics, mathematics, and simulation study, IEEE Transactions on Aerospace and Electronic Systems 42 (January (1)) (2006).

[3] X. Bai, F. Zhou, M. Xing, Z. Bao, High resolution ISAR imaging of targets with rotating parts, IEEE Transactions on Aerospace and Electronic Systems 47 (October (4)) (2011) 2530–2543.

[4] F. Totir, E. Radoi, Superresolution algorithms for spatial extended scattering centers, Digital Signal Processing 19 (September (5)) (2009) 780–792.

[5] M. Martorella, Novel approach for ISAR image cross-range scaling, IEEE Transactions on Aerospace and Electronic Systems 44 (1) (2008) 281–294.

[6] M. Martorella, F. Berizzi, Time windowing for highly focused ISAR image reconstruction, IEEE Transactions on Aerospace and Electronic Systems 41 (3) (2005) 992–1007.

[7] Y. Wang, Y.-C. Jiang, ISAR imaging of ship target with complex motion based on new approach of parameters estimation for polynomial phase signal, EURASIP Journal on Advances in Signal Processing 2011 (2011). Article ID 425203, 9 pp..

[8] T. Sparr, B. Krane, Micro-Doppler analysis of vibrating targets in SAR, IEE Proceedings Radar, Sonar and Navigation 150 (August (4)) (2003) 277–283.

[9] T. Thayaparan, S. Abrol, E. Riseborough, Micro-Doppler feature extraction of experimental helicopter data using wavelet and time-frequency analysis, in: RADAR 2004, Proceedings of the International Conference on Radar Systems, 2004.

[10] T. Thayaparan, S. Abrol, E. Riseborough, L. Stanković, D. Lamothe, G. Duff, Analysis of radar micro-Doppler signatures from experimental helicopter and human data, IET Radar, Sonar and Navigation 1 (August (4)) (2007) 288–299.

[11] J. Li, H. Ling, Application of adaptive chirplet representation for ISAR feature extraction from targets with rotating parts, IEE Proceedings Radar, Sonar and Navigation 150 (August (4)) (2003) 284–291.

[12] T. Thayaparan, P. Suresh, S. Qian, Micro-Doppler analysis of rotating target in SAR, IET Signal Processing 4 (3) (2010) 245–255.

[13] L. Stanković, T. Thayaparan, I. Djurović, Separation of target rigid body and micro-Doppler effects in ISAR imaging, IEEE Transactions on Aerospace and Electronic Systems 41 (October (4)) (2006) 1496–1506.

[14] T. Thayaparan, L. Stanković, I. Djurović, Micro-Doppler based target detection and feature extraction in indoor and outdoor environments, Journal of the Franklin Institute 345 (September (6)) (2008) 700–722.

[15] LJ. Stanković, T. Thayaparan, M. Daković, V. Popović-Bugarin, Micro-Doppler removal in the radar imaging analysis, IEEE Transactions on Aerospace and Electronic Systems, 49 (April (2)) (2013).

[16] A. Mitra, D. Kundu, Genetic algorithms based robust frequency estimation of sinusoidal signals with stationary errors, Engineering Application of Artificial Intelligence 23 (2010) 321–330.

[17] E. Lutton, P. Matrinez, A Genetic Algorithm for the Detection of 2D Geometric Primitives in Images, INRIA Robotique, Image et Vision, 2110, November 1993.

[18] K. S. Tang, K. F. Man, S. Kwong, Q. He, Genetic algorithms and their applications, IEEE Signal Processing Magazine, 13 (November (6)) (1996) 22–37.

[19] V.C. Chen, H. Ling, Time-Frequency Transforms for Radar Imaging and Signal Analysis, Artech House, Boston, USA, 2002.

[20] L.J. Stanković, T. Thayaparan, M. Daković, I. Djurović, Micro-Doppler and Moving Target Analysis using Time Frequency Analysis Techniques Research Report, 2005.

[21] I. Djurović, L. Stanković, J.F. Bohme, Robust L-estimation based forms of signal transforms and time-frequency representations, IEEE Transactions on Signal Processing 51 (July (7)) (2003) 1753–1761.

[22] J.H. Holland, Adaptation in Natural and Artificial Systems, University of Michigen Press, Ann Arbor, 1975.

[23] L. Stanković, A measure of some time–frequency distributions concentration, Signal Processing 81 (March (3)) (2001) 621–631.

[24] V. Popović, I. Djurović, L. Stanković, T. Thayaparan, M. Daković, Autofocusing of SAR images based on parameters estimated from the PHAF, Signal Processing 90 (May (5)) (2010) 1382–1391.

[25] I. Djurović, M. Simeunović, B. Lutovac, Are genetic algorithms useful for the parameter estimation of FM signals? Digital Signal Processing 22 (December (6)) (2012) 1137–1144.